Chemical Structure and Oxygen Dynamics in $Ba_2In_2O_5$

Stuart B. Adler, Jeffrey A. Reimer,* Jay Baltisberger, and Ulrike Werner

Contribution from the Department of Chemical Engineering and Department of Chemistry, University of California, Berkeley, Berkeley, California 94720-9989

Received August 6, 1993®

Abstract: Oxygen-17 magnetic resonance, in conjunction with high-temperature X-ray diffraction (XRD) and differential thermal analysis (DTA), were used to investigate the structure of $Ba_2In_2O_5$ and the dynamics of oxygen ion motion between room temperature and 1200 °C. NMR and thermal analysis demonstrate that at 925 °C there is an order–disorder transition which involves oxygen atoms between layers of octahedrally coordinated indium atoms. Both NMR and X-ray diffraction show that the material retains an orthorhombic (layered) structure until ~1075 °C, at which point the material becomes cubic. The number of mobile oxygen atoms in the structure increases continuously between 925 and 1075 °C, and only above 1075 °C does the full population of anions become mobile. These results imply that vacancies contribute to transport two-dimensionally within the tetrahedral layers at the order–disorder transition.

Introduction

Advanced ceramic materials are receiving increasing scientific and industrial attention because they show promise in a wide spectrum of applications, from automobile manufacturing to alternative energy technology. Nonstoichiometric oxides form one class of ceramics that appear to be excellent candidates for solid-state electrolytes, electrodes, electrocatalysts, and separation membranes.[1,2] Improved synthesis methods and recent discoveries of new materials have brought many of these applications within commercial grasp; however, fundamental understanding of these materials is still quite limited. In particular, since the properties of these materials derive both from their *long range order* and their *local structure*, they cannot be understood solely within the classic paradigms of condensed matter physics or modern chemical thermodynamics. Systematic understanding of these materials requires approaches that simultaneously address disparate length scales.

Oxygen ion transport is one property of oxides that may be exploited for commercial processes. Oxygen ion transport in many oxides has been shown to occur by diffusion or migration of oxygen ion *vacancies*, which become mobile at high temperature.[3,4] Information from NMR spin–lattice relaxation measurements on simple binary metal oxides may be combined with point-defect models to fully describe vacancy trapping and transport.[5,6] Nonstoichiometric oxides, however, have complex structures which cannot be understood simply in terms of point defects. In this paper we combine results from NMR techniques, which probe local structure and dynamics, with XRD, which probes long-range structure, in order to understand oxygen transport in $Ba_2In_2O_5$, a diamagnetic insulating oxide with a layered perovskite-related structure.

The hypothesized brownmillerite structure of $Ba_2In_2O_5$ at 25 °C is showen in Figure 1. The structure consists of alternating

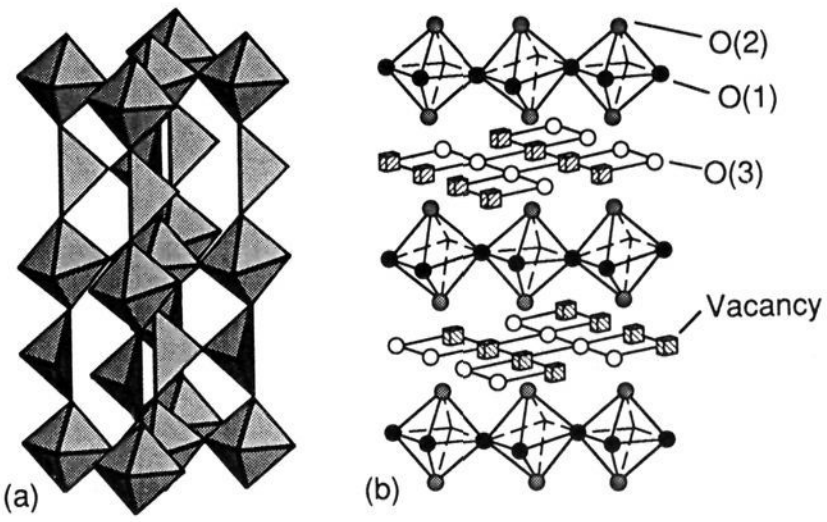

Figure 1. The hypothesized structure of $Ba_2In_2O_5$ based on its orthorhombic crystal symmetry: (a) the tilting arrangement of the InO_6 and InO_4 structural units; (b) the ordering of oxygen vacancies in layers of tetrahedrally coordinated indium atoms.

two-dimensional layers of corner-shared InO_6 octahedra and corner-shared InO_4 distorted tetrahedra. One way to classify this structure is as a cubic perovskite with a fixed concentration of oxygen ion vacancies that are ordered in two-dimensional planes. This ordering involves a cooperative tilting of the InO_6 octahedra in the octahedral layers and an ordered arrangement of the InO_4 tetrahedra in the tetrahedral layers such that vacancies lie in parallel chains. There are three crystallographically distinct oxygen sites: O(1) in the equatorial plane of the octahedra, O(2) at the apical sites of the octahedra and tetrahedra, and O(3) in the equatorial plane of the tetrahedra. This structure is discussed in greater detail in ref 8; it will become important later in the discussion to note that the O(3) site is a crystallographic inversion center.

Previous workers[3] have measured AC conductivity in this material from 25 to 1100 °C. A very interesting feature of their data is a discontinuous jump in the ionic conductivity by more than an order of magnitude at ~925 °C, which they have interpreted as an order–disorder transition of the vacancies in the structure. They imply that above the transition the material becomes a cubic perovskite in which all the vacancies are free to move among crystallographically equivalent oxygen sites.

In order to investigate the structure of $Ba_2In_2O_5$ and local dynamics of oxide anions, we have conducted several oxygen-17 NMR experiments with this material at temperatures between

* Abstract published in *Advance ACS Abstracts,* December 15, 1993.

(1) Kinoshita, K.; McLarnon, F. R.; Cairns, E. J. *Fuel Cell Handbook*; Lawrence Berkeley Laboratory Report, 1987.
(2) Steele, B. C. H. *Mater. Sci. Eng. B* **1992**, *13*, 79.
(3) Steele, B. C. H. Oxygen Ion Conductors. In *High Conductivity Solid Ion Conductors*; Takahashi, T., Ed.; World Scientific Publishing Co. Inc.: Teaneck, NJ, 1989.
(4) Kofstad, P. *Nonstoichiometry, Diffusion, and Electrical Conductivity in Binary Metal Oxides*; Robert E. Krieger Publishing Co., Malibar, FL, 1983.
(5) Adler, S. B.; Smith, J. W.; Reimer, J. A. *J. Chem. Phys.* **1993**, *98*, 7613.
(6) Adler, S. B.; Smith, J. W. *Faraday Trans. R. Soc.* **1993**, *89*, 3123.
(7) Goodenough, J. B.; Ruiz-Diaz, J. E.; Zhen, Y. S. *Solid State Ion.* **1990**, *44*, 21.
(8) Bertaut, P. E. F.; Blum, P.; Sagnieres, A. *Acta Crystallogr.* **1959**, *12*, 149.

0002-7863/94/1516-0675$04.50/0

25 and 1200 °C. These measurements, in conjunction with high-temperature X-ray diffraction (XRD) and differential thermal analysis (DTA), provide information about the onset and rate of oxide ion motion. The NMR and thermal analysis show that at 925 °C there is an order–disorder transition which involves the oxygen atoms in the tetrahedral layers. Both NMR and X-ray diffraction, however, show that the material retains an orthorhombic (layered) structure until ~1075 °C, at which point the material becomes cubic. The number of mobile oxygen atoms in the structure increases continuously between 925 and 1075 °C, and only above 1075 °C does the full population of anions become mobile. These results imply that at temperatures less than ~1000 °C vacancies become mobile only within tetrahedral layers and contribute to transport two dimensionally. The results have implications for the design of materials which attempt to exploit low-temperature oxygen anion mobility.

Experimental Section

Samples of $Ba_2In_2O_5$ were prepared by mixing and firing stoichiometric mixtures of $BaCO_3$ and In_2O_3 powders. The powders were mixed in a ball mill for 35 min and pressed into pellets at 20 kPa before firing at 1350 °C for 8 h in air. Following the initial synthesis, the pellets were reground and repressed before annealing at 1200 °C for 20 h, followed by an 8-h cool-down. Finally, the sintered pellets were reground to a fine powder before being enriched in ^{17}O by heating in water-free $^{17}O_2$ gas at 1 atm and 840 °C for 8 h. Comparison of the room temperature x-ray powder diffraction pattern to published diffraction data confirmed that the material was single-phase $Ba_2In_2O_5$.

Differential thermal analysis was performed using a Shimadzu TA-50 under flowing synthetic air (79% N_2, 21% O_2). High-temperature powder X-ray diffraction patterns were acquired at 750, 900, 1000, and 1200 °C in air on a Siemens Model D500 diffractometer equipped with a platinum-foil hot stage. The sample temperature was determined using a Pt–Pt/Rh thermocouple attached to the platinum sample holder. The diffraction patterns were acquired in order of decreasing temperature, and we waited approximately 1 h for thermal equilibration between experiments. The room temperature pattern was acquired separately on a different Siemens D500 diffractometer. All the patterns were indexed by hand to an orthorhombic or cubic unit cell.

Measurements of high-temperature oxygen-17 NMR were made using homebuilt NMR spectrometers, operating at 24.6 and 36.2 MHz (using 4.3- and 6.3-T superconducting magnets, respectively). The measurements were acquired using a water-cooled NMR probe which is a modification of a design described previously.[9] As demonstrated in Figures 2 and 3, the circuit stability of the probe allows direct comparison of nutation rates and signal intensities at different temperatures. One disadvantage of the water-cooled probe design is a relatively long acoustic "ringdown" time (50–100 μs), which places a lower limit on the ability to measure T_1 and T_2 accurately.

At high temperature, in the limit of motional narrowing of the resonance lines, spectra were obtained using single 90° pulses followed by a 70-μs ringdown period. At low temperature, where the line shape is generally dominated by second-order quadrupolar broadening,[10] spectra were obtained using a Hahn echo sequence appropriate to a pseudo spin $-^1/_2$, central transition line shape.[11] Nutation measurements were made by varying the length of the initial pulse in one of these two experiments. High-temperature measurements of the spin–spin relaxation time (T_2) were made by observing the decay of the signal as a function of the refocusing period in the Hahn echo sequence. Spin–lattice relaxation measurements (T_1) were made using an inversion–recovery sequence. The pulse sequences required for measuring these time constants are well-known and described elsewhere.[12] The integrated intensity of the spectra reported below were corrected for Curie law behavior and for T_2 decay during the Hahn echo.

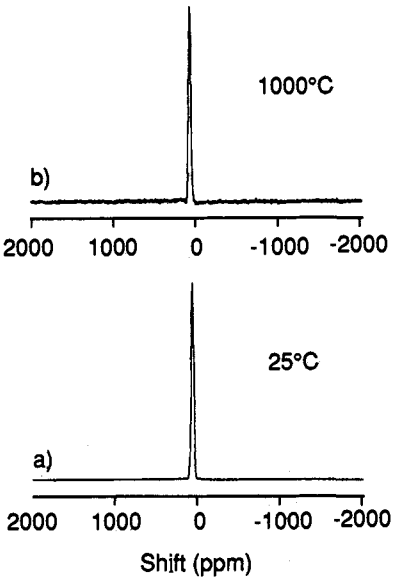

Figure 2. Oxygen-17 NMR spectra of MgO enriched to 25% in ^{17}O: (a) sample at 25 °C; (b) sample at 1000 °C. The integrated intensity of the high-temperature spectrum is within 40% of that of the low-temperature spectrum after correcting for Curie law behavior and differences in the spin–spin relaxation time. The line shape is independent of temperature and fits well to a Gaussian. Hole-burning experiments and estimates of the ^{17}O concentration both suggest that the line width is dominated by homonuclear dipolar coupling.

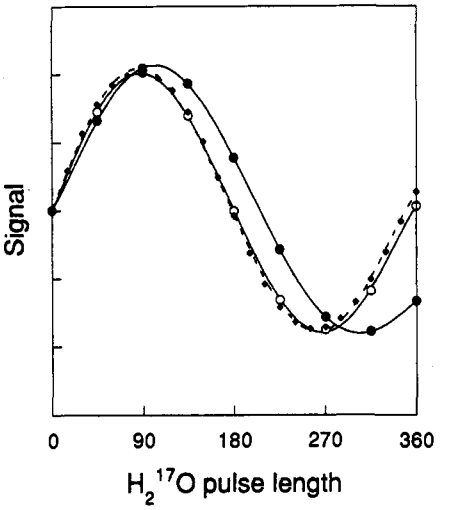

Figure 3. Nutation of the ^{17}O magnetization as a function of pulse length in the high-temperature probe: diamonds, the $H_2{}^{17}O$ reference by which pulse length is defined; open circles, nutation of $Mg^{17}O$ magnetization at room temperature; closed circles, nutation of $Mg^{17}O$ magnetization at 1000 °C. The decrease in nutation rate at 1000 °C reflects a 3% loss of circuit Q at the high temperature.

In order to remove spectral broadening from first-order and second-order anisotropies, room temperature magic angle spinning (MAS) spectra and dynamic angle spinning (DAS) were acquired, respectively. The data were obtained at 40.7 MHz using a Hahn echo for the MAS spectra and a 2-D hypercomplex shifted echo sequence for the DAS spectra. Information regarding the details of both these experiments can be found in ref 13–18.

(9) Adler, S. B.; Michaels, J. N.; Reimer, J. A. *Rev. Sci. Instrum.* **1990**, *61*, 3368.
(10) Taylor, P. C.; Baugher, J. F.; Kriz, H. M. *Chem. Rev.* **1975**, *75*, 203.
(11) Fukushima, E.; Roeder, S. B. *Experimental Pulse NMR*; Addison-Wesley: Reading, 1981; p 110.
(12) (a) Gerstein, B. C.; Dybowski, C. R. *Transient Techniques in NMR of Solids*; Academic Press: Orlando, 1985. (b) Ernst, R. R.; Bodenhausen, G.; Wokaun, A. *Principles of Nuclear Magnetic Resonance in One and Two Dimensions*; Oxford University Press, 1987.
(13) Mueller, K. T.; Sun, B. Q.; Chingas, G. C.; Zwaziger, J. W.; Terao, T.; Pines, A. *J. Magn. Reson.* **1990**, *86*, 470.
(14) Llor, A.; Virlet, J. *Chem. Phys. Lett.* **1988**, *152*, 248.
(15) Chmelka, B. F.; Mueller, K. T.; Pines, A.; Stebbins, J.; Wu, Y.; Zwanzinger, J. W. *Nature* **1989**, *339*, 42.
(16) Ganapathy, S.; Schramm, S.; Oldfield, E. *J. Chem. Phys.* **1982**, *77*, 4360.
(17) Lefebvre, F.; Amoureux, J.-P.; Fernandez, C.; Derouane, E. G. *J. Chem. Phys.* **1987**, *86*, 6070.

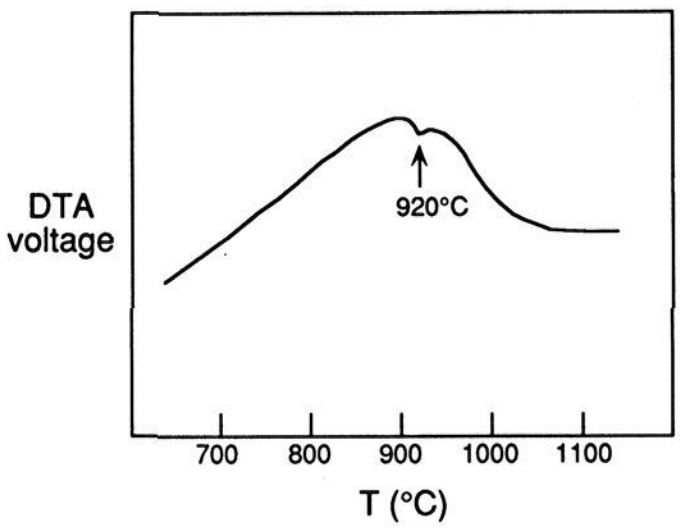

Figure 4. Differential thermal analysis (DTA) of $Ba_2In_2O_5$. The large roll in the data is a result of a miss-alignment of the detector and is present with blank test samples.

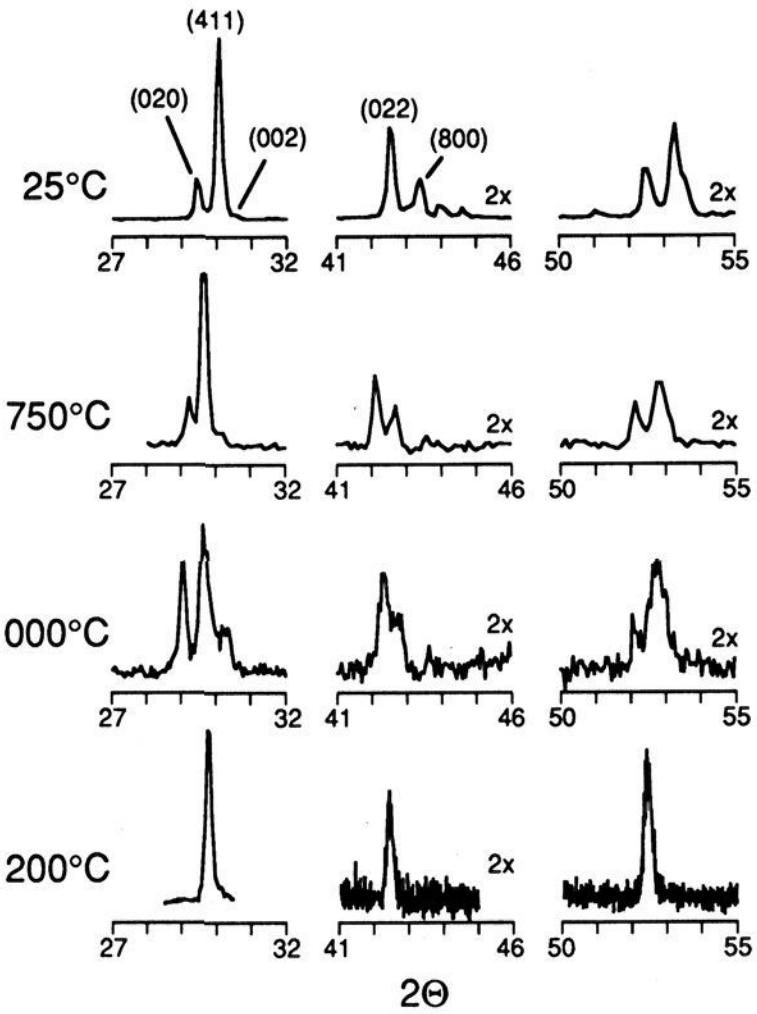

Figure 5. Variable-temperature X-ray diffraction of $Ba_2In_2O_5$. The signal intensities within each pattern are magnified as indicated.

Results and Analysis

X-ray Diffraction and Thermal Analysis. Figure 4 shows the DTA results obtained from $Ba_2In_2O_5$. In comparison to a platinum reference, there is a distinct endotherm at ~925 °C, the same temperature where previous workers have observed a jump in the ionic conductivity.[3] Thermogravimetric analysis over the same temperature range shows that this transition is not associated with a loss or gain of sample mass. This experiment shows, therefore, that there is an endothermic phase transformation associated with the sudden increase in oxygen ion transport.

Figure 5 shows the results of high-temperature X-ray powder diffraction obtained from $Ba_2In_2O_5$ at several selected diffraction angles. The patterns below 1200 °C index to an orthorhombic cell, indicating that the material retains a layered structure until at least 1000 °C. At 1200 °C the pseudocubic lines coalesce, suggesting a transition to cubic symmetry somewhere between 1000 and 1200 °C, a much higher temperature than the orthorhombic transition at 925 °C. The lack of a sharp transition in the DTA above 1000 °C suggests that this orthorhombic–cubic transition does not involve a discontinuous change of internal energy.

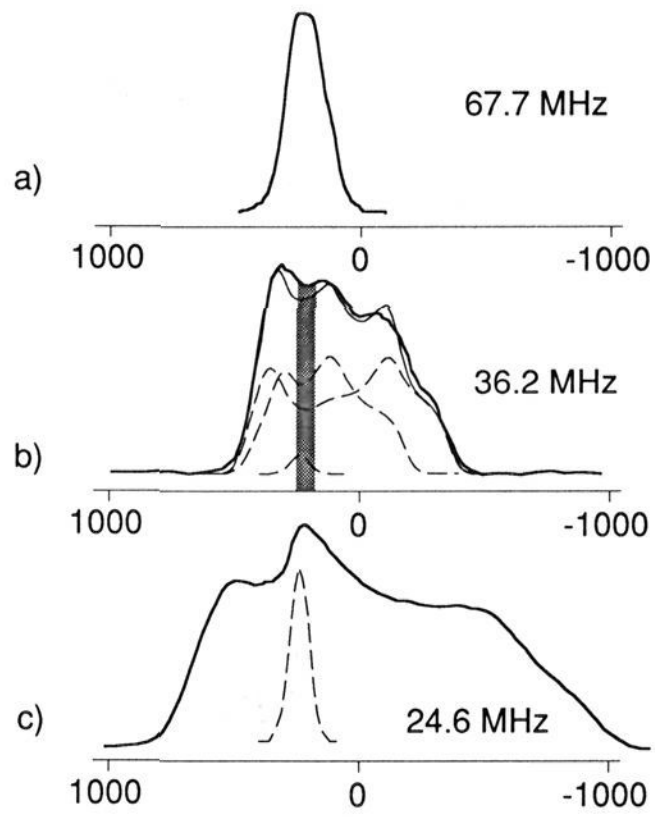

Figure 6. Room-temperature ^{17}O NMR spectra, in ppm, of $Ba_2In_2O_5$ at various magnetic field strengths. The spectrum shown in part b is fit to the sum of three line shapes: two second-order quadrupolar powder patterns {ω_Q = 7.8 MHz, η = 0.3; shift = 160 ppm; ω_Q = 6.9 MHz, η = 0.4, shift – 160 ppm} and a Gaussian {shift = 215 ppm}.

NMR at Room Temperature. Figure 6 shows room-temperature ^{17}O NMR spectra of $Ba_2In_2O_5$ acquired at different magnetic field strengths. The spectra show that the line width (in ppm) scales as the inverse square of the magnetic field, indicating that the spectra are broadened by the second-order quadrupolar interaction.[10] The 36.2-MHz data are well-simulated by two second-order quadrupolar powder patterns of roughly equal intensity. The DAS data presented in Figure 7b,c show two sharp resonances with isotropic second-order quadrupolar shifts consistent with the simulation parameters in Figure 6. The chemical shifts of these two resonances are between 150 and 200 ppm.

The third component in the line shape shown in Figure 6b becoms especially apparent in the 24.6-MHz spectrum, where the two quadrupolar powder patterns are broadest. Although this relatively narrow line shape is subject to modest first-order quadrupolar broadening (as evidenced by the presence of side bands in the MAS spectrum (Figure 7a), the sharpness of the line both with and without magic angle spinning indicates the absence of a strong second-order quadrupolar interaction. The absence of second-order quadrupolar broadening for this component is confirmed by the nutation data shown in Figure 8. The narrow line shape nutates at a rate equal to that of $H_2{}^{17}O$, while the two broad components nutate three times faster. This indicates that the narrow component, when irradiated with our spectrometer, is composed of all five of the 17-oxygen nuclear spin transitions.[11] *This nutation rate may only occur in the absence of quadrupolar* broadening.[10,12] The chemical shift of the narrow component is 220 ppm, similar to that of the other two components.

Given the evidence above, it is apparent that the narrow component of the line shape emanates from the O(3) site of $Ba_2In_2O_5$. The O(3) site is a crystallographic inversion center with cubic symmetry and therefore experiences no electric field gradients and hence no quadrupolar broadening. The other two components are heavily broadened by the second-order quadrupolar interaction and thus are associated with oxygen sites that have large electric field gradients owing to an asymmetric distribution of charge. We surmise, then, that these broad

(18) Grandinetti, P. J.; Baltisberger, J. H.; LLor, A.; Lee, Y. K.; Werner, U.; Eastman, M. A.; Pines, A. *J. Magn. Reson. Ser. A* **1993**, *103*, 72.

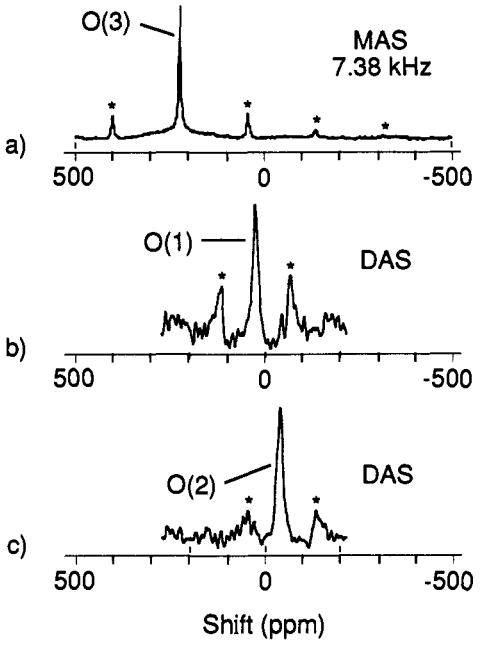

Figure 7. Room-temperature ^{17}O NMR spectra of $Ba_2In_2O_5$ under conditions of sample spinning. Side bands are marked with asterisks. (a) Magic angle spinning (MAS) at 8kHz. (b,c) Slices from a 2D hypercomplex shifted-echo dynamic angle spinning (DAS) experiment. No other resonances were found.

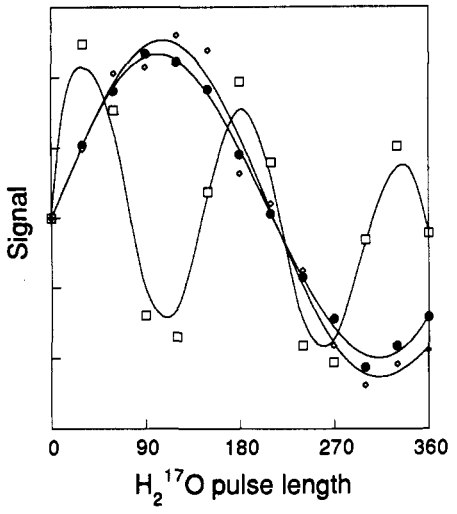

Figure 8. Nutation of the ^{17}O magnetization in $Ba_2In_2O_5$ as a function of $H_2{}^{17}O$ pulse length: diamonds, the narrow component of the ^{17}O line shape shown in Figure 6b with the sample at room temperature; squares, the second-order quadrupolar broadened components of the ^{17}O line shape shown in Figure 6b with the sample at room temperature; closed circles, the total ^{17}O line shape with the sample at 1060 °C.

components emanate from the O(1) and O(2) sites. Although the larger asymmetry parameter of the second peak seems most consistent with the O(2) site (which sits between octahedral and tetrahedral layers), one would need to perform careful single-crystal ^{17}O NMR measurements to differentiate between the quadrupolar parameters for the O(1) and O(2) sites. It is reasonable, however, that the chemical shifts of all three sites are similar since the charge densities around the oxygen nuclei are determined largely by cation valence in ionic materials.

NMR at 1200 °C. Figure 9 shows ^{17}O NMR spectra obtained from $Ba_2In_2O_5$ at 4.3 T (36.2 MHz) at temperatures ranging from room temperature to 1200 °C. The spectra narrow with increasing temperature, becoming a single Lorentzian peak at 1200 °C with a chemical shift intermediate among the three room-temperature values (210 ppm). At 1200 °C nutation

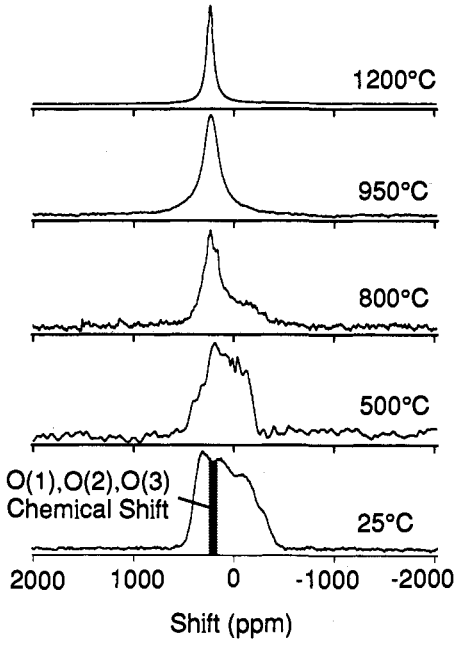

Figure 9. Variable-temperature ^{17}O spectra obtained from $Ba_2In_2O_5$.

measurements demonstrate that all five spin transistions are being irradiated, indicating the absence of a quadrupolar interaction. The signal intensity at 1200 °C is 10–15 times larger than that obtained at room temperature, indicating that all the nuclei in the sample can be observed.[19] The Lorentzian line shape suggests that the broadening of the line is due to a decay process, and indeed relaxation measurements at 24.6 MHz (discussed subsequentially) show that the line shape is primarily lifetime broadened.

One cannot explain the narrow line at 1200 °C as simply a consequence of the transition to cubic symmetry above 1000 °C. Although the material has overall cubic symmetry, there is local disorder due to partial occupancy of the oxygen sites: we expect a nonvanishing quadrupolar interaction even in the cubic phase. Indeed, loss of single and/or broadening of ^{17}O spectra due to local (vacancy-generated) electric field gradients has been observed in *cubic* yttria-doped CeO_2[20] and ZrO_2[21] at room temperature. The narrowness of the high-temperature ^{17}O spectrum from $Ba_2In_2O_5$, the appearance of all five spin transitions, the lifetime-broadened line shape, and the contribution of all the nuclei to the observed signal intensity indicate that the quadrupolar interaction is averaged away by rapid (≫36 MHz) motion of oxygen atoms between different oxygen sites.

NMR at Intermediate Temperatures. We may summarize the two temperature extremes as follows: at room temperature the material is condensed into the brownmillerite structure with no atomic motion on the NMR time scale. At 1200 °C the material is cubic with rapid (≫36 MHz) motion of all the oxygen nuclei between crystallographically equivalent oxygen sites. To understand what happens at intermediate temperatures we must examine carefully the complex behavior of the NMR spectra and relaxation rates between these two temperature extremes.

Figure 9 shows that there is a distinct drop in the signal intensity from the broad O(1) and O(2) components of the spectrum at intermediate temperatures. At lower field strengths (24.6 MHz)

(19) For a given number of nuclei, the integrated intensity of a spectrum which only involves the central transition has 1/12 the intensity of a spectrum in which all five transitions are present.[11] Since the room temperature spectrum of $Ba_2In_2O_5$ primarily involves the central transition only, we expect its intensity at room temperature to differ from the intensity at high temperature by a factor of about 12.

(20) Fuda, K. et al. *J. Phys. Chem. Solids* **1985**, *46(10)*, 1141.

(21) Adler, S. B. Masters Thesis, University of California at Berkeley, 1989.

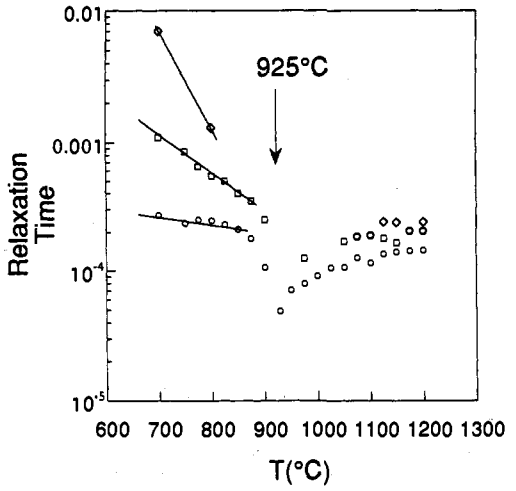

Figure 10. Values (in seconds) of the spin–lattice relaxation time (T_1, diamonds), the spin–spin relaxation time (T_2, squares), and the line widths (as $^*T_2$, circles) for the ^{17}O NMR signal in $Ba_2In_2O_5$. $^*T_2$ is defined as 2π/fwhm, where fwhm is the full width at half-maximum intensity of the line shape.

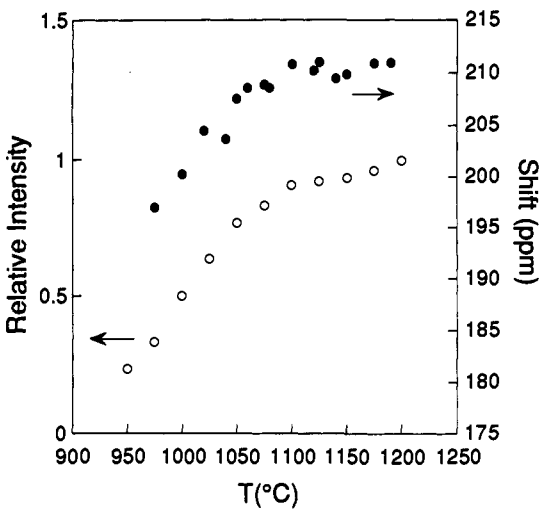

Figure 11. Integrated signal intensity and shift of ^{17}O resonance in $Ba_2In_2O_5$ at high temperatures. The intensity is corrected for Curie law behavior and for T_2 decay within the echo experiment used in acquiring the data.

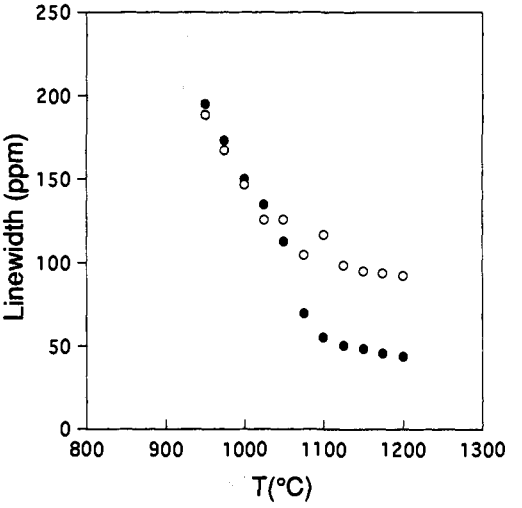

Figure 12. Line width of the ^{17}O spectra from $Ba_2In_2O_5$ as a function of temperature near 1075 °C. The line width is reported in parts per million of the applied field: open circles are data obtained at 4.3 T (24.5 MHz) and filled circles are data obtained at 6.3 T (36.2 MHz).

where the second-order quadrupolar broadening is strongest, only the narrow O(3) component of the line can be observed between 700 and 925 °C. A check of the nutation rate, integrated intensity, and chemical shift of this remaining signal confirms that it corresponds to the O(3) site. Since all spectra were acquired with Hahn spin echoes, the absence of contributions from the O(1) and O(2) sites implies that the spin–spin relaxation time, T_2, for the line shapes associated with the O(1) and O(2) sites became short relative to the echo delay time. Variation of this delay time (i.e., the time between the excitation pulse and the acquisition of the echo) confirms that above 500 °C, the T_2's of the line shapes associated with the O(1) and O(2) sites are less than 100 μs. This rapid loss of coherence indicates that the O(1) and O(2) sites experience kHz-frequency fluctuations of the second-order quadrupolar interaction. The T_2 of the narrow line shape associated with the O(3) site, however, remains much longer than the echo delay time throughout the 700 to 925 °C temperature range, thus indicating that the motion responsible for this relaxation does not involve exchange of atoms between the O(1) and O(2) sites and the O(3) site.

Although the O(3) site remains the only contributor to the 24.6-MHz spectrum between 700 and 925 °C, observation of the changes in the line shape above 700 °C provides information regarding structural dynamics of $Ba_2In_2O_5$. Figure 10 shows the reciprocal of the line width ($^*T_2$) along with measured values of T_2 and T_1 at selected temperatures. The line width is roughly independent of temperature below 850 °C and is best described as a Gaussian. Above 800 °C, however, the line shape acquires a Lorentzian shape, and the time constants $^*T_2$, T_2, and T_1 converge. The Lorentzian line shape and parallel behavior of these time constants with increasing temperature suggest that a substantial contribution to the line width is from lifetime broadening.

Above 850 °C the line width begins to broaden dramatically, and at 925 °C there is a sharp singularity in the line width. At that same temperature both T_1 and T_2 became too short to measure with our apparatus (i.e. T_1 and T_2 became less that the Hahn echo delay time, ~70 μs). These facts indicate that the line width becomes dominated by lifetime effects. The sharp minimum in the spin–lattice relaxation time at 925 °C cannot be explained by stochastic, activated motion near ω_0 because the minimum in the relaxation time is too sharp and localized in temperature;[22] our results suggest that a mode of motion is operative only near megahertz frequencies over this narrow temperature range. This singularity in relaxation time occurs at the same temperature as the endotherm in the DTA and the jump in the ionic conductivity.

Above 925 °C, the line shape narrows again, and continues to narrow with increasing temperature. Figure 11 shows that the intensity and shift rise continuously with temperature until ~1075 °C, where they level off to their maximum value. The change in signal intensity cannot be explained by an increasing satellite contribution to the observed signal because nutation measurements demonstrate that all five spin transitions already participate in the spectrum throughout this temperature range. Furthermore, increased satellite involvement would not produce changes in the chemical shift. The trends depicted in Figure 11 suggest that a growing number of oxygen nuclei from the O(1) and O(2) sites experience motional narrowing of the quadrupolar interaction, and thereby contribute to the observed spectra.

The leveling-off of the shift and the integrated intensity above 1075 °C suggests that the oxygen sites become equivalent. Further evidence for this can be seen in Figure 12, which shows a comparison between the line widths at 24.6 and 36.2 MHz. Below 1050 °C the line width (in Hz) scales with magnetic field, suggesting that the line width is substantially broadened by a

(22) Slichter, C. P. *Principles of Magnetic Resonance*, 3rd ed.; Springer Series in Solid-State Sciences; Springer-Verlag, 1989; Vol. 1.

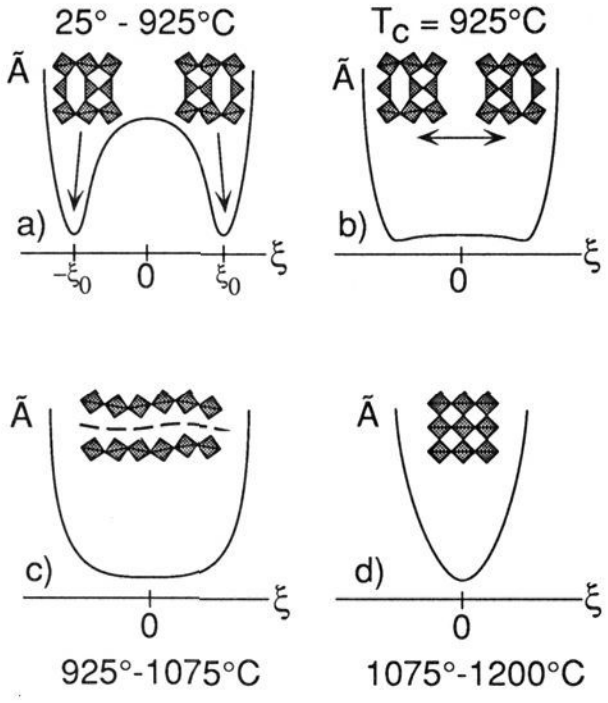

Figure 13. Schematic representation of $Ba_2In_2O_5$ structure and dynamics at high temperatures: (a) spontaneous cooperative ordering; (b) the critical temperature; (c) shrinking of structural fluctuations and spreading of disorder; (d) cubic structure with rapid isotropic motion of oxygen anions.

chemical shift distribution among the three oxygen sites. Above 1050 °C, however, the line width scales *inversely* with magnetic field, indicating the onset of a different broadening mechanism.[23] This disappearance of the chemical shift distribution strongly suggests that the oxygen sites in the material become equivalent on the NMR time scale due to rapid exchange among different oxygen sites.

Discussion

Figure 13 depicts a model for vacancy ordering and dynamics in $Ba_2In_2O_5$ that we believe is consistent with our NMR observations. We imagine defining an order parameter ξ which describes the ordering of the vacancies in the tetrahedral planes. In analogy to an Ising antiferromagnet, the ordering can be "positive" or "negative" depending on which "direction" the symmetry breaks at the time of spontaneous ordering. Let us further imagine that we can define a Helmholtz energy **A** which describes the probability of microstates with order parameter ξ. At low temperature (Figure 13a) the crystal can be in one of two states, ξ_0 or $-\xi_0$, with a large thermodynamic barrier in between. Because the structure is not symmetric, the displacement of vacancies requires cooperative motion of the entire structure from one state to the other, not just a local displacement of atoms. Displacement of an individual vacancy pays a large energetic penalty: as a result, there are few accessible states which can contribute to oxygen transport and concomitantly below 500 °C there is little detectable motion of oxygen atoms.

Between 500 and 925 °C there is a shortening of T_2 for the O(1) and O(2) sites, indicating the onset of kilohertz-frequency fluctuations of the second-order quadrupolar interaction. The spin–spin relaxation time for the remaining O(3) site, however, is much longer than that of the other two sites, indicating that there is little mixing of oxygen nuclei between the O(3) site and its neighbors on the kilohertz time scale. We conclude that while there must be structural fluctuations which produce a coherence loss for the O(1) and O(2) sites, this motion does not involve interchange among the different oxygen sites, nor does it disturb the cubic symmetry of the O(3) site. Since it is unlikely that the O(1) and O(2) sites can undergo mutual exchange without participation of the O(3) site, this motion must primarily involve structural fluctuations that do *not* contribute to oxygen transport. One possibility would be *local* cooperative inversion of the InO_6 octahedral tilts that modulates the O(1) and O(2) quadrupolar interaction (Figure 13b). Like a spin-flip in an Ising magnet, such a fluctuation cannot propagate at low temperature. Since any vacancy displacement that takes place as a result of the fluctuation is reversed when the fluctuation is extinguished, the ionic conductivity in this temperature range has a high Arrhenious slope, reflecting the large energetic penalty that must be paid to create effective charge carriers. This behavior continues until approximately 925 °C.

At 925 °C there is a singularity in the relaxation rate. Such singularities are commonly seen at order–disorder transitions in solids[24] and are caused by critical slowing down of phonon modes (soft phonons) to megahertz frequencies at the critical temperature.[25] Since this singularity occurs at the same temperature as both the endotherm in the DTA experiments and the jump in the ionic conductivity, we believe there is compelling evidence for an order–disorder transition in $Ba_2In_2O_5$. It is clear from the X-ray powder diffraction data, however, that the material is still orthorhombic until at least 1000 °C, indicating that vacancies do not disorder isotropically, as suggested previously.[3] Furthermore, if the vacancies became disordered isotropically throughout the sample at 925 °C, then one would expect the signal intensity above 925 °C to involve all the oxygen atoms in the sample. This is not the case as the signal intensity at 925 °C only involves the O(3) site. Although it is unclear from the data what the details of this order–disorder transition are, it is clear that below 1075 °C the motion of oxygen nuclei is not isotropic and that at the order–disorder transition there is little site exchange that involves atoms from the O(1) and O(2) sites. The chemical shift distribution implied by Figure 11 suggests that mixing does not occur at megahertz frequencies until the temperature is above 1075 °C.

On the basis of this behavior, we postulate that the order–disorder transition is best described by the model as shown in Figure 13b. We surmise that at the critical temperature (T_c) the free energy surface flattens and spontaneous, long-length-scale fluctuations between states ξ_0 and $-\xi_0$ become allowed. As a result of this flattening, phonon modes that normally operate on a time scale of 10^{-13} s acquire a significant density of states in the megahertz frequency range,[25] resulting in a singularity in the NMR relaxation rate. We suspect that these fluctuations involve long waves of cooperative octahedral tilt inversions that travel through the crystal, allowing vacancy displacement within the tetrahedral layers. As a result, the signal from the O(3) site, which is involved in these vacancy displacements, becomes lifetime broadened. An endotherm in the DTA appears as these new degress of freedom become active; there is also a jump in the ion conductivity as a result of two-dimensional vacancy transport within the tetrahedral layers. This vacancy transport, however, does not involve oxygen atoms between the tetrahedral layers; the cooperative tilt inversions responsible for vacancy displacement only require the bending of the In–O(1)–In and In–O(2)–In bond axes, not exchange with the O(1) and O(2) sites.

The most interesting feature of this transition is that it does not involve a change of global crystal symmetry. X-ray diffraction shows that this material is still orthorhombic above 925 °C, suggesting that the long-length-scale structural fluctuations that occur at the critical temperature must be larger that the length scale detected by XRD (~30 nm). If structural microdomains were significantly smaller than this, one would observe a cubic or at least tetragonal average structure. The vacancies are thus ordered in a time-averaged sense; snapshots of the structure (as

(23) A Lorentzian line shape that narrows with increasing field is characteristic of lifetime broadening near a T_1 minimum. The flat relaxation behavior in Figure 10 above 1100 °C is consistent with the system being near a T_1 minimum.

(24) Rao, C. N. R.; Rao, K. J. *Phase Transitions in Solids*; 1st ed.; McGraw-Hill: New York, 1977.

(25) An excellent discussion of this subject can be found in: Rigamonti, A. *Adv. Phys.* **1984**, *33*, 115.

acquired by XRD) show that the instantaneous state of the system is ordered over long length scales. Long-length-scale fluctuations are a common characteristic of systems near their critical points; however, the highly cooperative dynamics in this system appear to cause fluctuations that extend over almost macroscopic dimensions. As the temperature is raised further (Figure 13 c), motional narrowing spreads beyond the tetrahedral layers and participation of NMR signal from atoms in sites O(1) and O(2) becomes significant. Finally at 1075 °C and above (Figure 13d), the material becomes cubic with isotropic vacancy motion among all oxygen sites. The continuous changes in the shift and signal intensity between 925 and 1075 °C, as well as the absence of discontinuities in the DTA or ion conductivity at 1075 °C, suggest that this transformation to cubic symmetry is much gentler than the order–disorder transition at 925 °C. In fact the only evidence we have for a discontinuous transition is the change in line width at 36.2 MHz, as shown in Figure 11. Since the exchange of oxygen between the octahedral and tetrahedral site is probably activated, the suddenness of the change in line width could easily be explained on kinetic grounds.

One possible explanation for the absence of a phase transition at 1075 °C is that the only difference between the material at 1000 and 1200 °C is the length scale over which structural fluctuations occur. The instantaneous local structure at 1200 °C cannot be cubic because of the large concentration of disordered vacancies; perhaps these vacancies are ordered in the high-temperature phase on a length scale too small to be observed by X-ray diffraction. If this were true then isotropic behavior observed at 1200 °C is actually an average which results from rapid, short-length-scale structural fluctuations. This scenario would be consistent with the observation that many other perovskites with cubic crystal structures have short-length-scale noncubic microdomains which largely determine their properties.[26] A more complete study of high-temperature XRD between 925 and 1075 °C might shed further insight as to how this evolution to cubic symmetry takes place.

Conclusions

The experimental results presented support the conclusion that an order–disorder transition occurs among the vacancies in $Ba_2In_2O_5$ at 925 °C. Both NMR and X-ray diffraction, however, show that the material retains an orthorhombic (layered) structure until ~1075 °C, where the material becomes cubic. The number of mobile oxygen atoms in the structure increases continuously between 925 and 1075 °C, and only above 1075 °C does the full population of anions become mobile. These results imply that vacancies become mobile primarily within the tetrahedral layers at the order–disorder transition, and contribute to transport two-dimensionally.

Our results for $Ba_2In_2O_5$ may be extrapolated to issues relating to the systematic design of oxide materials for oxygen transport. Optimization of vacancy concentration and/or local vacancy hopping kinetics are not sufficient to systematically maximize oxygen ion transport. Thermodynamic considerations such as the dynamics associated with structural phase transitions in nonstoichiometric oxides appear to play a crucial role in determining vacancy and concomitantly oxygen ion transport.

Acknowledgment. The authors would like to acknowledge useful discussions with Steve Russek and Angelica Stacy. The authors are also grateful to Y. Wu for the spectrum shown in Figure 6a and to Phil Grandinetti and Alex Pines for their assistance with sample spinning experiments. J.A.R. is a Camille and Henry Dreyfus Teacher-Scholar. Some facilities used in this work were provided by the Director, Office of Basic Sciences, Materials Sciences Division of the U.S. Department of Energy under Contract No. DE-AC03-765F00098.

(26) Adler, S. B. Ph.D. Thesis, University of California, Berkeley, 1993.